Astronomy Reports, Vol. 47, No. 12, 2003, pp. 979–988. Translated from Astronomicheskiĭ Zhurnal, Vol. 80, No. 12, 2003, pp. 1064–1074.
Original Russian Text Copyright © 2003 by Vasil'Ev, Shchekinov.

The Formation of the First Objects During the Virialization of the Dark-Matter Halo

E. O. Vasil'ev and Yu. A. Shchekinov

Physics Department, Rostov State University, Rostov-na-Donu, Russia

Received September 30, 2002; in final form, July 26, 2003

Abstract—The chemical and thermal evolution of the baryon component in the gravitational field of low-mass primordial dark-matter halos during their virialization is studied. We consider low-mass halos to be those for which the characteristic baryon cooling time can appreciably exceed the co-moving Hubble time, so that the cooling process can continue to the current epoch ($z \sim 0$). The virialization process is described in two scenarios: "quiet " virialization, in which the establishment of the virial state is assumed to be homogeneous over the entire volume considered, and "violent" virialization, in which the establishment of the virial state is assumed to be realized via the action of shock waves. In this second case, the efficiency of the formation of molecular hydrogen grows substantially, and can reach $H_2/H \sim 0.01$ in some cases, which exceeds current estimates by at least an order of magnitude. This eases the condition for the birth of the first gravitationally bound objects with comparatively low masses ($M \gtrsim 2 \times 10^5 M_\odot$), possibly leading to an appreciable increase in the fraction of the mass going into Population III objects, and also to a shift in the onset of the formation of the first stars toward higher redshifts. © *2003 MAIK "Nauka/Interperiodica"*.

1. INTRODUCTION

One of the key questions in modern cosmology is the nature of the first stellar objects: their masses, the epoch of their formation, and their evolutionary status. The properties of these first objects determine the entire subsequent evolution of the Universe, and their influence on the ionization state of diffuse gas determines the level of angular fluctuations in the cosmic background radiation. In cosmological models with cold dark matter, the formation of the first stellar objects corresponds to the compression of baryonic matter in the gravitational field of non-baryonic dark matter, which forms, in turn, so-called dark halos—condensations of dark matter in a virial state [1]. The minimum mass of the first objects can be estimated as the minimum baryonic mass that can not only sustain itself in the gravitational field of the dark halo, but also be compressed, with the subsequent formation of gravitationally bound condensations of baryons—future protostars or proto-stellar clusters.

This question has been studied by a number of groups in recent years, and the following scenario is currently generally accepted [2] (see also the reviews [3, 4]). Let us consider a mass M consisting nearly 90% of non-baryonic dark matter that separates out from the general Hubble expansion and reaches a virial state at redshift z_v. The temperature of the baryons associated with the mass M in the virial state reaches some value $T_v(M)$ that depends on M [5]:

$$T_v \cong 0.3 \left(\frac{\pi^3}{96}\right)^{1/3} \frac{G\mu m_p}{k} M^{2/3} (\Omega_m \rho_0)^{1/3} (1+z), \tag{1}$$

where $\rho_0 = 3H_0^2/8\pi G$ is the critical density. If gas at this temperature is able to cool via radiative losses in molecular hydrogen lines at the given z, it can subsequently contract and form a gravitationally bound baryonic object. Since the efficiency of the formation of H_2 molecules and cooling via their line radiation falls off with decreasing temperature, there exists at each z a minimum mass $M_m(z)$ for which the gas at the temperature T_v ends up in a cooling state over the co-moving Hubble time $t_{\rm H}(z)$: $M_m(z)$ is a decreasing function of z [2]. The absolute minimum mass of the first objects and the epoch of their formation in the Universe z are determined by the intersection of the mass $M_m(z)$ and the mass of the halo $M_{3\sigma}(z)$ corresponding to a fluctuation amplitude exceeding the 3σ level. According to [2], this redshift is $z = 30$, and the masses of the first objects were $M \sim 10^6 M_\odot$. Only objects with higher masses can form at lower redshifts. The cooling criterion adopted in [2] is that there be a substantial decrease in the temperature of the gas compared to the virial temperature over some specified time for each z: all objects satisfying the condition $T(\eta z) < \eta T(z)$ with $\eta = 0.75$ are considered to be cooling, and capable of further forming gravitationally bound baryonic systems.

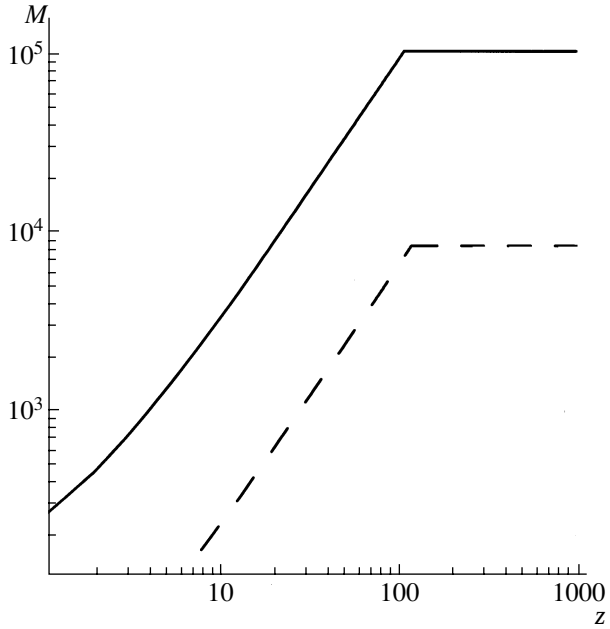

Fig. 1. Jeans mass M_J (solid curve) and the minimum mass M_c (dashed curve) in units of $M_\odot$.

Thus, this scenario is limited to rapidly evolving gas condensations that preferably form the earliest stellar systems at redshifts close to the epoch when the halo separates out from the Hubble expansion. In addition, objects with lower masses that evolve appreciably more slowly remain outside this framework, so that they become capable of forming stellar systems only at epochs close to the current epoch ($z \sim 0$), or alternatively form metal-poor gravitationally bound clumps that are captured by more massive galaxies in a bottom—up heirarchical scheme for galaxy formation.

In the current paper, we follow the evolution of such low-mass, cooling baryonic condensations over fairly long time intervals, often appreciably exceeding the co-moving Hubble time. This enables us to distinguish a class of first-generation objects (i.e., those born from primordial material), whose formation extends to comparatively low redshifts, or, in some cases, even to the current epoch, so that the epochs of their formation can coincide with the formation of objects of subsequent generations, which were born from material that has already been enriched in metals. Being gravitationally bound, such objects will be essentially isolated, and will not become enriched in metals. Therefore, they could supply material for dwarf galaxies with extremely low metal abundances at the current epoch [6].

Another important circumstance of the scenario described above is that we have excluded from consideration the specific process by which the dark halos are virialized, supposing only that this virialization is accomplished via violent relaxation on time scales appreciably shorter than the co-moving Hubble time. (In models of violent relaxation, the characteristic virialization time for a dark halo differs from the co-moving Hubble time by the factor $\sqrt{\langle\rho\rangle/\rho_h}$, where $\langle\rho\rangle$ is the mean total density in the Universe and ρ_h is the mean density of the halo.) In addition, the process of violent relaxation proceeds with the appearance of appreciable fluctuations of the temperature and density of the relaxing system [7, 8]. In the case of a mixture of baryon and dark components, the situation is complicated by the fact that, being dissipative, the baryon component can form a structure during the virialization process; i.e., generally speaking, long before the dark-matter component reaches the virial state. A full description of this process requires three-dimensional numerical simulations of a two-fluid, self-gravitating medium, and is accordingly extremely computationally intensive. In the current paper, we propose a qualitative analysis of the chemical and thermal evolution of the baryon component based on a simple model for the virialization of dark halos. A more detailed description of the fluctuations of the potential and density, as well as the results of two-dimensional numerical computations, will be given in subsequent papers. We present here the results of computations for a model with cold, dark matter and a Λ term (a ΛCDM model) with $\Omega = 1$, $\Omega_m = 0.29$, $\Omega_b = 0.047$, $\Omega_\Lambda = 0.71$, Hubble constant $h = 0.72$, and $\sigma = 0.9$ [9], although we also carried out computations for a standard CDM model with $\Omega = \Omega_m = 1$, $\Omega_b = 0.06$, Hubble constant $h = 0.5$, and $\sigma = 0.7$. The resulting minimum masses in the CDM model exceed those in the ΛCDM model by no more than a factor of two.

Section 2 describes the model underlying our analysis of the role of shock waves in the chemical and thermal history of the baryons in the virialization process. In Section 3, we formulate the equations used to study the dynamics of colliding baryonic condensations. In Section 4, we present a simple system of equations to describe the dynamics of the halos after they reach the virial state in a "quiet" virialization model. Section 5 describes the thermal and chemical processes determining the thermal evolution of the baryons. Finally, Sections 6 and 7 present our main results and conclusions.

2. DESCRIPTION OF THE VIRIALIZATION MODEL

The simple description of the processes determining the masses of the first objects in the Universe that we present here is based on certain assumptions about the virialization of dark-matter halos, including

the character of motions within them. In this section, we present arguments supporting these assumptions, and specify the initial state of baryons in the early stages of formation of gravitationally bound objects.

2.1. Model for the Virialization of Dark Halos

The formation and virialization of massive halos can be viewed as the unification of less massive into more massive fragments (subhalos), with subsequent relaxation to a new equilibrium corresponding to the higher mass. If an even more massive halo forms via the separation of a uniform (homogeneous) mixture of baryons and dark matter, the subsequent violent relaxation is accompanied by the formation of inhomogeneities in the cold component of the dark matter due to gravitational instability, whose interactions with each other accelerate the relaxation process. Following the terminology adopted in [7], we will call this model "violent" virialization, in constrast to the "quiet" virialization considered below (see Sections 4 and 6.1). In our simple description, we will assume that, at the time of its separation from the Hubble flow and the onset of virialization, a dark-matter halo of mass M consists of an ensemble of subhalos with lower masses m_i, such that $M = \sum_i m_i$. Even if the relative velocities of the lower-mass halos were initially small, they can grow during the subsequent compression of the system as a whole, reaching values close to $v_r \sim \sqrt{GM/r}$, where r is the current radius of the halo, and thus can exceed the virial velocity $v_R = \sqrt{GM/R}$ before equilibrium is attained, where R is the radius of the system in the virial state.

2.2. Critical Mass

We restrict our consideration to those stages of evolution of the Universe when the thermal contact between matter and radiation via Compton interactions between electrons and photons had ceased to be important. This corresponds to redshifts $z < z_i$, where

$$1 + z_i = 137 \left(\frac{\Omega_b h^2}{0.022}\right)^{2/5}, \qquad (2)$$

where $h = H_0/100$ km s^{-1} Mps^{-1} is the Hubble constant and Ω_b is the baryonic density parameter. At $z > z_i$, the temperature of baryons and electrons T coincides with the temperature of the background relict radiation $T_r = 2.7(1+z)$ K, while at $z < z_i$,

$$T_b = T_r \left(\frac{1+z}{1+z_i}\right)^2. \qquad (3)$$

In spite of the fact that the masses of dark halos are not restricted from below by gravitational instability (this restriction can be associated only with the possible cutoff of the perturbation spectrum $\delta_d(k)$), there is a critical mass below which baryons with the temperature $T_b(z)$ cannot be sustained by dark halos. We determine this critical mass by requiring that the virial temperature $T_v(M)$, which must be provided by the gravitational potential of the dark matter with mass M, be higher than the background temperature of the baryons (3): $T_v(M) > T_b(z)$. We thus obtain for the critical mass

$$M_c(z) \qquad (4)$$
$$= \begin{cases} 8.45 \times 10^3 M_\odot, & z > z_i, \\ 8.45 \times 10^3 M_\odot (1+z/1+z_i)^{3/2}, & z \le z_i. \end{cases}$$

Note that this value differs from the critical Jeans mass for the baryons $M_J(z)$, determined for the background baryon density and temperature. Figure 1 shows the dependences $M_c(z)$ and $M_J(z)$.

2.3. Criteria for Violent Relaxation and Virialization of the Halos

In the virial state, the outer radius of the halo is

$$R = \left(\frac{M}{24\pi^3 \Omega_m \rho_0}\right)^{1/3} (1+z)^{-1}, \qquad (5)$$

so that the characteristic velocity of the subhalos is

$$v_R = \sqrt{GM^{2/3}(24\pi^3\Omega_m\rho_0)^{1/3}(1+z)}. \qquad (6)$$

In our model for violent relaxation, the virial state is achieved via Coulomb scatterings of the halos on each other, with the interval between scatterings being

$$t_C = \left(\frac{3\pi}{2^9}\frac{N_s r^3}{G m_i}\right)^{1/2} [\ln(N_s/\sqrt{\pi})]^{-1}. \qquad (7)$$

We will consider the system to be relaxing if t_C is less than the co-moving Hubble time for a specified z and $t_C < t_{\rm H}(z)$. This corresponds to the condition

$$\frac{N_s}{\ln(N_s/\sqrt{\pi})} = \frac{2^7\pi}{3H_0}(G\rho_0)^{1/2}. \qquad (8)$$

It is easy to see that condition (8) yields $N_s < 3$ in the ΛCDM model with $\Omega_m = 0.29$. It is reasonable to suppose that, in the simplest case, halos of cold, dark matter virialize via the development of a dipolar mode corresponding to the oncoming motion of two flows, as occurs in the theory of the evolution of adiabatic perturbations of Zeldovich [10]. Thus, as a basic violent-relaxation model, we will consider a head-on collision of two flows (two subhalos) with masses $M_1 = M_2 = M/2$ and with velocities in the center-of-mass system equal to the virial velocities (6).

An important circumstance here is that, being collisionless, the dark matter leaves the region of shock

compression of the baryons. The oncoming flows of dark matter that arise are subject to bunching instability, which can bring about a rapid relaxation of the system to the virial state, and also facilitate the fragmentation of the compressed baryonic layer.

We also investigated shocks associated with the head-on collisions of lower-mass subhalos ($m_i < M/2$). However, since these subhalos will have the same characteristic velocity (6), while the durations of the collisions between them will be shorter, $\propto {m_i}^{1/3}$, the number of H_2 molecules in the final state is smaller, and consequently the efficiency of the cooling of the gas is lower.

3. BARYONS BEHIND THE SHOCK FRONTS

When considering models for violent virialization, we restricted our analysis to a one-dimensional description of the thermal evolution of the baryons during a collision of subhalos. The legitimacy of this approach is based on the fact that, since the gas flows are subsonic behind the front, expansion in the transverse direction (parallel to the plane of the shock front) requires more time than expansion in the direction of the collision. However, we should keep in mind that the development of a strong outflow of matter in the equatorial direction (along the shock front) immediately after the collision can lower the pressure behind the front, and consequently decrease the degree of compression and the efficiency of forming molecular hydrogen. However, as a rule, this decrease in pressure does not exceed a factor of two, so that our results will provide a qualitatively correct description of the dynamics of the cooling gas in colliding subhalos. In the absence of significant thermal conductivity, the evolution of the baryons behind the shock front can be described by a system of ordinary differential equations written for an individual Lagrange element of the fluid. We will assume that the temperatures of the electrons and heavy particles (atomic hydrogen and helium and their ions) coincide behind the front. In this case, the system of dynamical equations describing the thermal properties and chemical transformations of the baryon component behind the shock front during a collision of subhalos takes the form

$$\dot{T} = -\sum_i \Lambda_i(T, x_2, x, n), \tag{9}$$

$$\dot{x} = I(T, x, n) - R(T, x, n), \tag{10}$$

$$\dot{x}_2 = F(T, x, n) - D(T, x, n), \tag{11}$$

where Λ_i is the cooling rate of the gas associated with process i, I and R are the ionization and recombination rates for hydrogen (we neglect here the contribution of helium to thermal and ionizational processes), F and D are the total rates of the formation and dissociation of molecular hydrogen, x is the degree of ionization, x_2 is the relative number density of H_2, and T is the temperature of the gas. We assume that each gas element behind the front evolves isobarically, and describe the density using the expression

$$n = \frac{p}{\mu k T}, \tag{12}$$

$\mu = \rho/n m_p = 1.4$. Here, we have neglected the contribution of electrons, protons, and other particles taking part in the chemical and ionization equilibrium behind the front, since their relative number densities always remain substantially lower than unity. The pressure p is determined from the condition of conservation of momentum at the discontinuity:

$$p = \frac{15}{9}\rho_i v^2 \tag{13}$$

for an adiabatic shock, where v is the velocity of the cloud relative to the center of mass, ρ_i is the density of baryons in the subhalos before their collision, and

$$p = \rho_i v^2 \tag{14}$$

for a radiative shock [11]. We adopt for the initial temperature the temperature of the gas behind the shock front:

$$T_0 = \frac{15}{36}\frac{m_p}{k}v^2, \tag{15}$$

for an adiabatic shock and

$$T_0 = \frac{m_p}{4k}v^2, \tag{16}$$

for a radiative shock. The initial degree of ionization and number density of H_2 were taken to be equal to their cosmological values.

4. BARYONS IN THE QUIET VIRIALIZATION MODEL

The system of dynamical equations that we will use to describe the dynamics of the baryons in the field of the dark-matter halo in the case of quiet (spherically symmetrical) virialization can be written

$$\dot{R} = u, \tag{17}$$

$$\dot{u} = \frac{5}{11}\left[\frac{4kT}{\mu m_p R} - \frac{4}{3}\pi G(\rho_d + \rho)R\right], \tag{18}$$

$$\dot{T} = -\frac{2m_p}{3k}\left[\frac{3kT}{\mu m_p R} + \frac{4}{5}\pi G(\rho_d + \rho)R\right]u - \frac{2L}{3k\mu n}, \tag{19}$$

where $n = \rho/\mu m_p$, G is the gravitational constant, R the radius of the cloud, and u the velocity of the cloud particles at its boundary. The system (17)–(19) is

obtained from the integral form of the gas-dynamical equations [12]

$$\int_V \rho \mathbf{v} dV + \int_{t_0}^{t} dt \int_{\mathbf{S}} \rho v^2 d\mathbf{S} \tag{20}$$

$$= -\int_{t_0}^{t} dt \int_{\mathbf{S}} p d\mathbf{S} + \int_{t_0}^{t} dt \int_V \mathbf{F} dV$$

$$\int_V \rho(\epsilon + v^2/2) dV - \int_{V_0} \rho(\epsilon + v^2/2) dV \tag{21}$$

$$= -\int_{t_0}^{t} dt \int_{\mathbf{S}} p\mathbf{v} d\mathbf{S} - \int_{t_0}^{t} dt \int_V L dV + \int_{t_0}^{t} dt \int_V \mathbf{F}\mathbf{v} dV.$$

For a spherical cloud, substituting the thermodynamical quantities in the integrals with their mean values and assuming that the local velocity of the compression is proportional to the local radius (which, strictly speaking, is valid for a free-fall regime), $v(r) = -\alpha r$. In these equations, L [erg cm^{-3} s^{-1}] is the radiative-cooling rate per unit volume, $F(r) = -GM\rho/r^2$, $p = knT$, and $\epsilon = 3kT/2\mu m_p$. In the system made up of (17)–(19) and (20)–(21), it is assumed that the kinetic energy of the compressed gas is transformed into thermal energy on short timescales. It can readily be seen from (18)–(19) that, in the absence of radiative cooling, $L \equiv 0$, the gas temperature increases to the virial temperature as it is compressed, T_v (1), after which the rate goes to zero, and the compression ceases.

We solved the system (17)–(19) for a model with quiet evolution of the halo, without including the effects of fluctuations and the appearance of shocks. We considered the evolution of the baryon component from the time the dark halo separated out; i.e., from the turning point when the Hubble expansion within some perturbed region of dark matter is replaced by compression. We described the evolution of the dark matter using the approximate expression given in [2], which reproduces well the exact solution. We used the temperature and density corresponding to the turning point as their initial values, also taking the initial densities of electrons and H_2 molecules to be equal to their cosmological values at that time. The system of dynamical equations for the baryons (17)–(19) was solved further for the case of a specified (approximated) dark-matter background.

5. THERMAL AND CHEMICAL PROCESSES

The main cooling agents for the baryons in the redshift range of interest to us ($z < 200$) are molecular hydrogen, H_2, and HD. In the computations, we

Rates of chemical reactions

Reaction	Reaction coefficient k, cm^3 s^{-1}	Reference
$H^+ + e^- \to H + h\nu$	$k_1 \approx 1.88 \times 10^{-10} T^{-0.64}$	[16]
$H + e^- \to H^- + h\nu$	$k_2 \approx 1.83 \times 10^{-18} T^{0.88}$	[16]
$H^- + H \to H_2 + e^-$	$k_3 \approx 1.3 \times 10^{-9}$	[17]
$H^+ + H \to H_2^+ + h\nu$	$k_5 \approx 1.85 \times 10^{-23} T^{1.8}$	[18]
$H_2^+ + H \to H_2 + H^+$	$k_6 \approx 6.4 \times 10^{-10}$	[19]
$D^+ + H_2 \to HD + H^+$	$\alpha_1 \approx 2.1 \times 10^{-9}$	[15]
$H^+ + HD \to H_2 + D^+$	$\alpha_2 \approx \alpha_1 e^{-465K/T}/4$	[15]

adopted for the cooling function of the H_2 molecules [13] the expression

$$L_{H_2} \simeq \frac{{L_r}^E}{1 + n_{cr}/n}, \tag{22}$$

where the critical density is

$$n_{cr} \equiv \frac{{L_r}^E}{{L_r}^{(n\to 0)}} n, \tag{23}$$

which depends only on the temperature, not on n. The cooling rate in LTE is

$${L_r}^E \simeq \frac{1}{n}\left\{\frac{9.5 \times 10^{-22} {T_3}^{3.76} e^{-(0.13/T_3)^3}}{1 + 0.12 {T_3}^{2.1}} + 3 \times 10^{-24} e^{-0.51/T_3}\right\} \text{эрг см}^3/\text{с}, \tag{24}$$

while the cooling rate in the limit of low densities is

$${L_r}^{(n\to 0)} \simeq \frac{5}{4}\gamma_2 (E_2 - E_0) e^{-(E_2 - E_0)/kT} + \frac{7}{4}\gamma_3 (E_3 - E_1) e^{-(E_3 - E_1)/kT}. \tag{25}$$

Here, $T_3 = T/1000\ K$ and $E_J = J(J+1)E_1/2$, where $E_1/k \simeq 171\ K$, and γ_2 and γ_3 are the collisional de-excitation rates for transitions from the $J = 2$ and $J = 3$ rotational levels [13]:

$$\gamma_J = \left(\frac{10^{-11} {T_3}^{1/2}}{1 + 60 {T_3}^{-4}} + 10^{-12} T_3\right) \times \left\{0.33 + 0.9 \exp\left[-\left(\frac{J - 3.5}{0.9}\right)^2\right]\right\} \text{ cm}^3/\text{s}. \tag{26}$$

Equation (25) assumes that the ratio of the ortho and para configurations of H_2 is 3 : 1. The first and second terms give the contributions to the cooling from para- and ortho-H_2. It is shown in [14] that, in the volume reactions

$$H_2(\text{orto}) + H^+ \to H_2(\text{para}) + H^+, \tag{27}$$

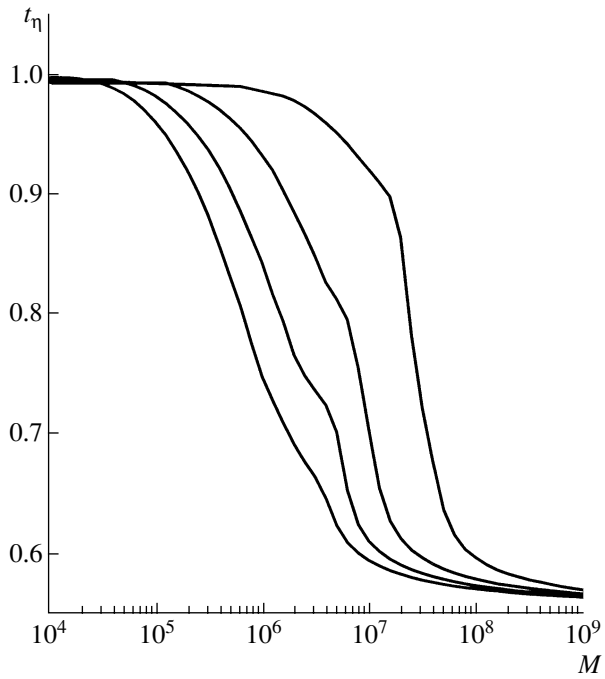

Fig. 2. $t_\eta(M)$ relation, where t_η is the time that has passed from the separation of the halo from the cosmological expansion to the collapse ($\eta = 10$) in units of the comoving Hubble time $t_{\rm H}(z)$, for $z_v = 40...10$ in steps of ten (left to right). For low masses, this time is comparable to the current age of the Universe. The masses are indicated in units of $M_\odot$.

all the ortho-H_2 is transformed into para-H_2. Thus, the corresponding cooling rate is obtained by multiplying the first term of (25) by four; i.e., Eq. (25) is replaced by the simpler expression

$$L_r{}^{(n\to 0)} \simeq 5\gamma_2(E_2 - E_0)e^{-(E_2-E_0)/kT}. \qquad (28)$$

For the rate of cooling by the HD molecules, we adopted the expression [13]

$$L_{\rm HD} = 6.6\times 10^{-23}T^{-1/2} \times \exp\left(-\frac{128.4{\rm K}}{T}\right)\ {\rm erg\,cm^3/s}. \qquad (29)$$

The critical density for the HD molecules is substantially higher than the values attained in our computations. The computations included the chain of reactions presented in the table, which are the dominant processes under the conditions considered. A very complete analysis of the reactions in a primary gas is presented in [15]. We neglected the contribution of the photodissociation of H^- and H_2^+ ions by photons of the background radiation, since their energies are two to three orders of magnitude lower than the binding energies of these ions in the redshift range considered, $z \le 40$.

Taking into account the fact that the reactions $D^+ + H_2 \longrightarrow HD + H^+$ and $H^+ + HD \longrightarrow H_2 + D^+$ are rapid, i.e., their characteristic time scales are substantially shorter than other time scales in the problem, the system of equations describing the relative densities of electrons $x = n_e/n$ and H_2 molecules, $f = 2n(H_2)/n$, can be written

$$\dot{x} = -k_1 n x^2, \qquad (30)$$

$$\dot{f} = 2k_m n(1 - x - f)x, \qquad (31)$$

where, in accordance with [2] and allowing for the fact that photodissociation of the H^- and H_2^+ ions by cosmic background photons is negligible,

$$k_m = k_2 + k_5, \qquad (32)$$

(the first and second terms describe the formation of H_2 in reaction chains involving the H^- ion and H^+ ion, respectively). The collisional ionization of H atoms and dissociation of H_2 are negligibly small under the low-temperature conditions we are considering.

At temperatures below $\simeq 400$ K, the effect of the chemical fractionation of deuterated molecular hydrogen becomes important [20]. In late stages of the compression of the condensations as the gas is cooled to a temperature of ~ 30 K, all the deuterium may be transformed into molecular form [21]. However, under the conditions for the initial evolution of the halos considered here, when the temperature of the baryons is not able to fall below $30 - 100$ K, the contribution of HD molecules to the thermal balance is only 5–10%.

6. RESULTS

6.1. Model for Quiet Virialization

At each fixed redshift, we carried out computations for grids of halo masses exceeding the critical mass $M_c(z)$, and determined the minimum mass $M_m(z)$ for which the baryons are able to be cooled and compressed. The computations were conducted for a standard CDM model and for a CDM model with a Λ term. The standard CDM model gives minimum masses that exceed their values for the ΛCDM model by no more than a factor of two. We fixed the baryon mass, taking it to be equal to $(\Omega_b/\Omega_m)M$, where M is the total mass of the cloud, including the baryon and dark matter components. Following the standard approach (see, for example, [2, 22]), we suppose that, at some z, a perturbed region separates out from the general Hubble expansion, begins to be compressed, and, at $z \simeq z_v$, the halo of dark matter relaxes to the virial state with characteristic density

$$\rho_v \approx 18\pi^2\rho_0\Omega_d(1+z)^3, \qquad (33)$$

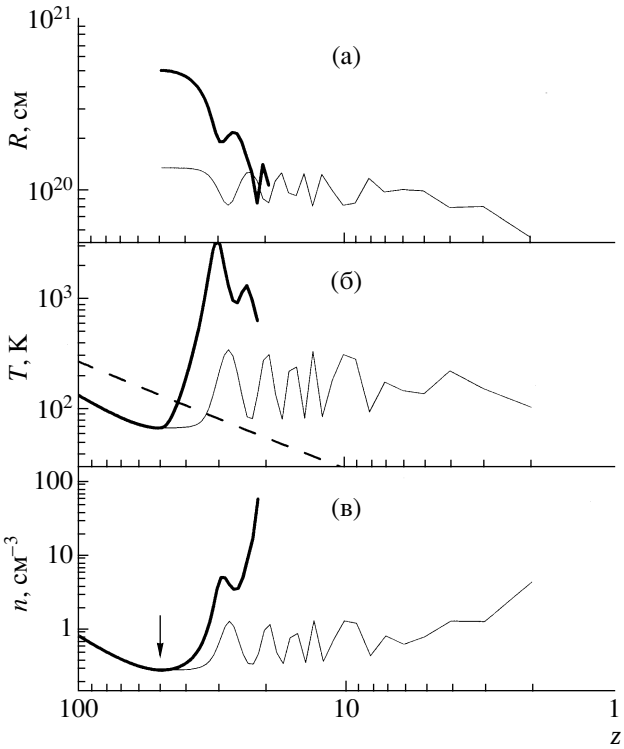

Fig. 3. Evolution of the (a) radius, (b) temperature, and (c) density for two types of halos (with masses close to and appreciably exceeding the critical mass, shown by the dotted and solid curves, respectively) that have become virialized at $z_v = 30$. The time of the separation from the cosmological expansion is indicated by the arrow. The middle graph also shows the temperature of the cosmic background radiation (dashed curve).

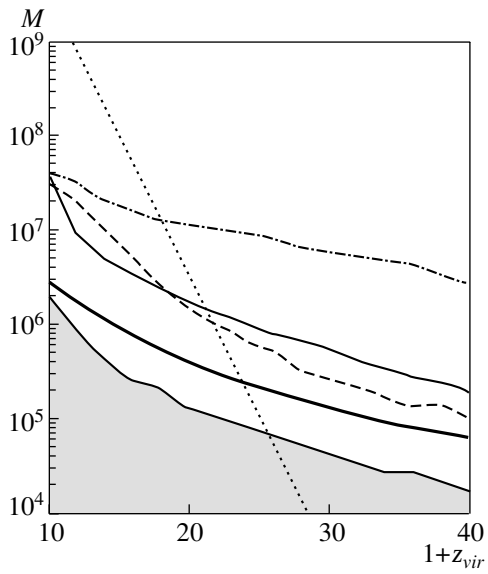

Fig. 4. Minimum mass required for collapse. Only masses lying above the shaded region can be compressed and form objects by the current age of the Universe (slowly evolving objects). Masses lying above the thin, solid curve can be compressed and form objects over the local (at the time of virialization) Hubble time (rapidly evolving objects corresponding to the compression criterion [2]). The thin, dot–dash curve corresponds to rapidly evolving objects satisfying our compression criterion. The thin, dotted curve corresponds to objects forming by the epoch $z = 6$. The bold, solid curve shows the minimum masses for rapidly evolving objects in a violent-virialization scenario. The dashed curve corresponds to 3σ fluctuations in the ΛCDM model ($\sigma_8 = 0.9$). The masses are indicated in units of $M_\odot$.

where $\Omega_d = \Omega_m - \Omega_b$. We used the following approximation to describe the transition to the virial state in the computations [2]:

$$\rho(z) \approx \rho_0 \Omega_d (1+z)^3 \exp\left(\frac{1.9A}{1-0.75A^2}\right), \quad (34)$$

where

$$A(z) \equiv \frac{1+z_v}{1+z}. \quad (35)$$

We assumed that the density of baryons in the halo varies proportional to the density of dark matter before the separation from the Hubble expansion, after which we found the solution to the system of equations (17)–(19). Thus, in contrast to [2], we separate the evolution of the baryon component from the non-baryon component at stages following the separation from the cosmological expansion. As a criterion for the formation of a gravitationally bound baryonic object, we adopted the condition that, in the process of the cooling and compression of the baryon component in the total gravitational field of the baryons and dark matter, the density of baryons within the radius occupied by the baryon component must exceed the density of the non-baryonic dark matter by a specified factor $\eta > 1$. This is a stricter condition than the condition that the temperature of the baryons decrease by a factor of 1.5, as was adopted in [2]. Figure 2 shows the $t_\eta(M)$ dependence, where t_η is the time that has passed from the separation from the cosmological expansion to the final compression (when $\eta > 1$) in units of the co-moving Hubble time $t_{\rm H}(z)$ for various z_v.

Figure 3 depicts the evolution of the radius, temperature, and density for two values of z_v for two types of halos: those with masses close to and much greater than the critical mass $M_c(z)$. There are obvious differences in the evolution of these halos. In the former case, molecular hydrogen forms slowly in the compressed baryon component, so that only after several oscillations does enough H_2 accumulate to provide the subsequent cooling and monotonic compression of the baryons. In the latter case, a sufficient quantity of H_2 forms even in the initial stages of the compres-

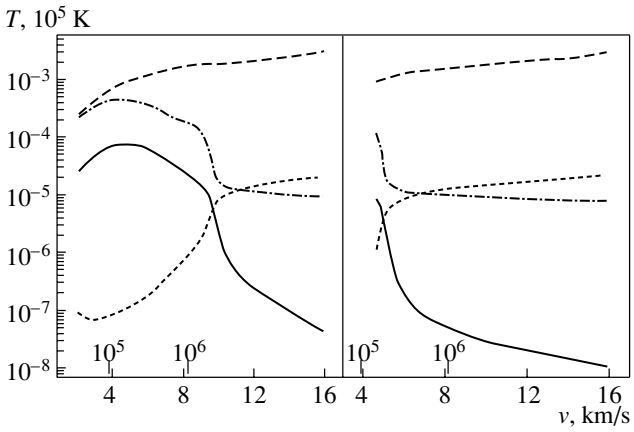

Fig. 5. Dependences of the number densities of electrons, molecular hydrogen, and HD and of the baryon temperature (solid, dashed, dotted, and dot–dash curves, respectively) on the halo collision velocity for head-on collisions. The masses of the halos are $M_s = 10^4 M_\odot$ (left plot) and $M_s = 10^5 M_\odot$ (right plot). The marks below indicate the virial velocities corresponding to the indicated series of masses (in units of $M_\odot$).

sion, giving rise to the rapid cooling and compression of the baryon component. For each z_v, we computed the dynamics of the compression of an ensemble of halos with various masses, in order to find the critical (minimum) mass $M_m(z)$ of a halo that is able to be compressed over the local (i.e., modern) Hubble time. These masses lie above the shaded region in Fig. 4, which also shows the minimum mass for rapidly (over the co-moving Hubble time) evolving halos for the criterion applied in [2] (solid, thin curve; the computations in [2] were carried out for the standard CDM model, while we have recomputed the results of [2] for a ΛCDM model), and for our stricter criterion (thin, dot–dash curve; corresponding to the rapid compression of the baryons to $M_b/M_d > 1$ over the co-moving Hubble time). We can see that the differences in the masses for rapidly and slowly evolving halos can reach two orders of magnitude. The thin dashed curve corresponds to masses that are compressed and form gravitationally bound baryonic condensations by the epoch $z = 6$ in our model. The upper limit for the mass of the baryonic objects being born is determined by the curve $M_{3\sigma}$, which corresponds to exceeding the density fluctuations at the 3σ level [4] (dashed curve in Fig. 4). Thus, gravitationally bound objects with a wide range of masses $M_m(z) < M < M_{3\sigma}(z)$ are simultaneously born and evolve in the Universe. The more massive objects evolve more rapidly, while lower-mass objects can give rise to new stellar systems only at later epochs.

6.2. Model for Violent Virialization

In accordance with the above, we also carried out computations for each fixed redshift for a grid of halo masses M in this model. The halos relaxed via the collision of two subhalos with half the total mass, $M_s = M/2$, and with the virial velocities in the center-of-mass system:

$$v_R \cong 1.16 \times 10^5 \left(\frac{M}{10^6\, M_\odot}\right)^{1/3} (1+z)^{1/2}\ \text{см/с}. \tag{36}$$

The computations were conducted for collisional velocities from 2 to 16 km/s, which corresponds to the virial velocities for halo masses $M = (2 \times 10^4 – 8 \times 10^6) M_\odot$ at redshift $z = 30$.

A halo was considered to be capable of subsequently forming a stellar system if the Jeans mass in the cooled gas after the collision was smaller than the total mass of the baryons. The corresponding halo mass is shown by the bold solid curve in Fig. 4. The computations were carried out over times equal to one dynamical time for the colliding subhalos: $t_d = R/v$. This corresponds to the fact that the compressed object will begin to expand and the formation of H_2 molecules will cease at $t > t_d$. Figure 5 presents the dependence of the number densities of the electrons, H_2, and HD and of the temperature on the velocity of the subhalo collisions at redshift $z = 30$, for $M_s = 10^4 M_\odot$ (left) and $M_s = 10^5 M_\odot$ (right). The mass of a halo (in $M_\odot$) for which the virial velocity is equal to the corresponding velocity on the x axis is shown below.

We expect that, in a more complex scenario when the relaxation of the halos occurs due to interactions between multiple (more than two), less massive subhalos, the formation of H_2 molecules and the cooling due to them will be less efficient than in the case considered above, since the times for their interactions will be shorter, $t_d \propto m_i^{1/3}$. Note, however, that the final count at time $t = t_d$ corresponds to a lower limit to the effects discussed, since, after a collision, the expanding gas fragments take part in subsequent collisions with fragments from other collisions, with the characteristic relative velocities being $\sqrt{2} v_R$. As a result, a random, supersonic velocity and density field that is close to a logarithmic normal distribution will be established in the system, as follows from numerical simulations [23]. One consequence of this will be the ongoing, more efficient formation of H_2 molecules behind the shock front, enhancing the overall cooling of the baryon component of the halo.

6.3. Survival of Low-mass Objects

A fundamental question is the survival of slowly evolving objects in the field of the ionizing radiation created by the stellar population born from rapidly evolving systems with high masses (above the limit of [2], shown by the thin solid curve in Fig. 4). One of the most important consequences of the formation of the first objects is the secondary ionization and heating of the Universe [4, 9, 24–27]. The subsequent evolution of protogalaxies and the efficiency of star formation in them can be substantially affected by the ionizing radiation emitted by the first objects formed. We note in this connection that the most recent observations of distant quasars with redshifts $z \gtrsim 4.5$ as part of the Sloan Digital Sky Survey appear to indicate that the secondary ionization and heating occurred near redshifts $z \sim 6$, so that the flux of ionizing radiation drops sharply at high redshifts ($z > 6$), as is testified to by the latest observations of the Gunn–Peterson effect [28–30] and the WMAP data [9]. This may indicate that the very first objects in the Universe formed low-mass stars that were not able to make an appreciable contribution to ionizing radiation, that the bulk of the ionizing photons are trapped in denise zones of HII, or alternatively that the number of these earliest objects was small. In any case, this means that low-mass (slowly evolving) objects with masses in the interval indicated above can evolve without being appreciably affected by ionizing radiation, at least to redshifts $z \sim 6$. Indeed, at the densities that are reached in these objects at stages when the central baryon density exceeds the density of the non-baryonic dark component by an order of magnitude, the number density of hydrogen is $n \sim 10\ \mathrm{cm}^{-3}$. At ionization rates $\xi_{\mathrm{H}} < 4 \times 10^{-14}\ \mathrm{s}^{-1}$, corresponding to redshifts $z > 6$ [30], the degree of ionization brought about by external radiation is only $x < 4 \times 10^{-2}$, and the ionization induced heating rate is $\Gamma \lesssim 6 \times 10^{-26}\ \mathrm{erg\ s}^{-1}$, while the rate of cooling by molecular hydrogen at these stages lies in the range $\sim (4–6) \times 10^{-26}$ for masses of $(0.3–3) \times 10^6 M_\odot$, which virialize at $z = 30–20$. The rate of dissociation of H^- ions by ionizing radiation of the Lyman continuum for the flux estimated in [30] is $\sim 4 \times 10^{-18}\ \mathrm{s}^{-1}$, substantially lower than the rate at which they are transformed into H_2 ($\sim 10^{-8}\ \mathrm{s}^{-1}$). Note that, under these conditions, the ionizing radiation can stimulate the formation of H_2 if it leads to an enhancement of the electron density to $x \sim 10^{-2}$. In the more realistic case of violent relaxation of the halos with the formation of multiple shocks, the efficiency of the secondary ionization and photodissociation of H_2 decreases, because the density of gas in regions through which the shocks have passed is higher than the average density. Thus, we expect that some low-mass halos can be preserved in the external field of ionizing radiation, and, moreover, some fraction of these can subsequently also contribute to this field. It will be possible to draw firm conclusions only on the basis of self-consistent computations of the formation of the first stellar objects and the production of ionizing radiation by them.

7. CONCLUSIONS

(1) We have considered the evolution of low-mass, slowly evolving first objects—so-called dark-matter halos, which give rise to the first stellar population of the Universe. We showed in our simple (quiet) virialization model that baryonic objects with masses exceeding $(0.3–10) \times 10^5 \Omega_b M_\odot$ can be compressed and give rise to stellar systems at the current epoch. Baryonic objects with masses $(0.1–12) \times 10^6 \Omega_b M_\odot$, which virialize at $z = 40–10$, form gravitationally bound systems by $z = 6$. Since the mass function of the first objects decreases with the mass (probably more rapidly than M^{-1}), this may mean that the production of ionizing photons at $z < 6$ will be higher than is usually predicted.

(2) We have shown that the estimated minimum mass of the forming objects depends substantially on the adopted baryon-cooling criterion. In particular, if we take such objects to be those in which the baryons are compressed during the cooling process to densities exceeding the density of dark matter in the central regions of the halo, then this state can be reached over the co-moving Hubble time only by objects whose masses exceed the known limit [2] by half an order of magnitude.

(3) We have examined the influence of the shock waves that necessarily arise during the virialization of the halos on the thermal regime of the baryons in a simplified approach. The minimum baryon temperature is achieved during collisions of fragments with masses that are half the mass of the halo. Although the fraction of such halos is probably small, precisely they give rise to the formation of the least massive first objects, with masses $(0.6–12) \times 10^5 M_\odot$, which is lower than the limit of [2] by a factor of 2–12.

8. ACKNOWLEDGEMENTS

The authors thank the referee for comments. This work was supported by the Russian Foundation for Basic Research (project code 00-02-17689) and the State Science and Technology Program "Astronomy" (project 1.3.1.1).

REFERENCES

1. M. J. Rees and J. P. Ostriker, Mon. Not. R. Astron. Soc. **179**, 541 (1977).
2. M. Tegmark, J. Silk, M. J. Rees, *et al.*, Astrophys. J. **474**, 1 (1997).
3. D. Galli, F. Palla, *H_2 in Space*, Ed. by F. Combes and G. Pineau des Forêts (Cambridge, Cambridge University Press, 1999), p. 41.
4. R. Barkana and A. Loeb, Phys. Rept. **349**, 125 (2001).
5. A. Blanchard, D. Valls-Gabaud, and G. A. Mamon, Astron. Astrophys. **264**, 365 (1992).
6. T. X. Thuan, Yu. I. Izotov, and V. A. Lipovetsky, Astrophys. J. **477**, 661 (1997).
7. D. Lynden-Bell, Mon. Not. R. Astron. Soc. **136**, 101 (1967).
8. F. H. Shu, Astrophys. J. **225**, 83 (1978).
9. D. N. Spergel, L. Verde, H. V. Peiris, *et al.*, Astrophys. J. (2003, in press); astro-ph/0302209.
10. Ya. B. Zel'dovich, Astrofizika **6**, 119 (1970).
11. A. A. Suchkov, Yu. A. Shchekinov, and M. A. Edel'man, Astrofizika **18**, 629 (1982).
12. L. D. Landau and E. M. Lifshitz, *Hydromechanics* (Moscow, Nauka, 1986).
13. D. Hollenbach and C. F. McKee, Astrophys. J., Suppl. Ser. **41**, 555 (1979).
14. T. Abel, P. Anninos, Y. Zhang, and M. L. Norman, New Astron. **2**, 181 (1997).
15. D. Galli and F. Palla, Astron. Astropys. **335**, 403 (1998).
16. J. B. Hutchins, Astrophys. J. **205**, 103 (1976).
17. T. Hirasawa, Progr. Theor. Phys. **42**, 523 (1969).
18. P. R. Shapiro and H. Kang, Astrophys. J. **318**, 32 (1987).
19. Z. Karpas, V. Anicich, and W. T. Huntress, J. Chem. Phys. **70**, 2877 (1979).
20. V. K. Khersonskiĭ and D. A. Varshalovich, Pis'ma Astron. Zh. **3**, 506 (1977) [Sov. Astron. Lett. **3**, 277 (1977)].
21. Yu. A. Shchekinov, Pis'ma Astron. Zh. **12**, 499 (1986) [Sov. Astron. Lett. **12**, 211 (1986)].
22. P. J.E. Peebles, *Principles of Physical Cosmology* (Princeton, Princeton Univ. Press, 1993).
23. P. Padoan, R. Jimenez, and B. Jones, Mon. Not. R. Astron. Soc. **285**, 711 (1997).
24. T. Abel and Z. Haiman, *H_2 in Space*, Ed. by F. Combes and G. Pineau des Forêts (Cambridge, Cambridge University Press, 1999), p. 237.
25. Z. Haiman and A. Loeb, Astrophys. J. **483**, 21 (1997).
26. A. Ferrara, Astrophys. J. **499**, L17 (1998).
27. B. Ciardi, A. Ferrara, and T. Abel, Astrophys. J. **533**, 594 (2000).
28. S. G. Djorgovski, S. Castro, D. Stern and A. A. Mahabal, Astrophys. J. **560**, L5 (2001).
29. X. Fan, V. K. Narayanan, M. A. Strauss, *et al.* Astron. J. **123**, 1247 (2002).
30. A. Lidz, L. Hui, M. Zaldarriaga, and R. Scoccimarro, Astrophys. J. **579**, 491 (2002).

Translated by D. Gabuzda